

Single-carrier Distributed Antenna Network Downlink Using Joint Transmit/Receive Diversity

Ryusuke MATSUKAWA[†] Tatsunori OBARA[†] Kazuki TAKEDA[†] and Fumiyuki ADACHI[‡]

Dept. of Electrical and Communication Engineering, Graduate School of Engineering, Tohoku University
6-6-05 Aza-Aoba, Aramaki, Aoba-ku, Sendai, 980-8579 Japan

E-mail: [†]{matsukawa, obara, kazuki}@mobile.ecei.tohoku.ac.jp, [‡]adachi@ecei.tohoku.ac.jp

Abstract—Single-carrier distributed antenna network (SC-DAN), in which a group of multiple antennas are distributed in a cell serve a user, can mitigate adverse impacts of path loss, shadowing loss and multipath fading. Frequency-domain space-time block coded-joint transmit/receive diversity (FD-STBC-JTRD) is attractive for downlink transmission since an arbitrary number of distributed transmit antennas can be used. FD-STBC-JTRD requires the channel state information (CSI) only at the transmitter side and therefore, the complexity problem of mobile terminals can be alleviated. In this paper, we investigate, by computer simulation, the bit error rate (BER) distribution of the SC-DAN downlink. We discuss the impact of the number of distributed antennas involved in FD-STBC-JTRD on the BER outage probability.

Keywords—component; Distributed antenna network, space-time block coding, frequency-domain equalization

I. INTRODUCTION

Broadband wireless channel is composed of many propagation paths having different time delays and hence becomes a severely frequency-selective [1]. The bit error rate (BER) performance of single-carrier (SC) transmissions is seriously degraded due to strong inter-symbol interference (ISI). This ISI problem can be overcome by the use of receive frequency-domain equalization (FDE). The minimum mean square error based FDE (MMSE-FDE) can take advantage of channel frequency selectivity and obtain large frequency diversity gain [2], [3]. Recently, transmit FDE has been attracting an attention [4], [5]. For further improving the transmission performance, the use of antenna diversity is effective. Joint use of antenna diversity and receive FDE is powerful for improving the signal transmission performance in a frequency-selective channel [6-8]. Recently, authors have proposed a frequency-domain space-time transmit diversity (FD-STTD) combined with receive FDE [9] and frequency-domain space-time block coded-joint transmit/receive diversity (FD-STBC-JTRD) combined with transmit FDE [10-12]. FD-STBC-JTRD requires channel state information (CSI) at the transmitter and can use an arbitrary number of transmit antennas while FD-STTD requires the CSI at the receiver and can use an arbitrary number of receive antennas. This suggests that if FD-STBC-JTRD and FD-STTD are applied to the downlink and uplink transmissions, respectively, the complexity problem of mobile terminals (MTs) will be

alleviated while using an arbitrary number of antennas at the base station.

In cellular mobile communications network, the received signal power varies due to changes in path loss and shadowing loss according to the user's movement [13]. Even if joint antenna diversity/FDE is used, the BER drops sometimes below an acceptable level. This problem becomes more pronounced when a user is near the cell edge. Distributed antenna network (DAN) is a promising network that can solve the problems arising from the path loss and shadowing loss [14-16]. Figure 1 illustrates a conceptual structure of DAN. In DAN, the conventional base station is replaced by the signal processing center (SPC) and many antennas are spatially distributed around the SPC. Each of distributed antennas is connected to the SPC by optical fiber link. Distributed antennas close to the MT cooperatively serve the MT using transmit diversity technique to mitigate the problem arising from path loss and shadowing loss. It was shown in [15] that DAN improves the spatial distribution of signal-to-noise interference ratio (SINR) compared to the conventional cellular network.

In this paper, we consider an SC-DAN downlink transmission using FD-STBC-JTRD. This network can obtain a fairly large diversity gain by using as many distributed antennas as possible while keeping the MT receiver's complexity low. We investigate, by computer simulation, the BER distributions of the SC-DAN downlink transmission. We also discuss the impact of the number of distributed antennas serving to a user and the propagation channel parameters on the BER outage probability.

The remainder of the paper is organized as follows. Sect. II introduces the SC-DAN model and the propagation channel model. Sect. III describes FD-STBC-JTRD for SC-DAN downlink transmissions. Section IV presents computer simulation results on the downlink BER distributions and discusses the impacts of the number of distributed antennas involved in FD-STBC-JTRD and the propagation channel parameters on the outage probability. Finally, Sect. V offers some conclusions and future works.

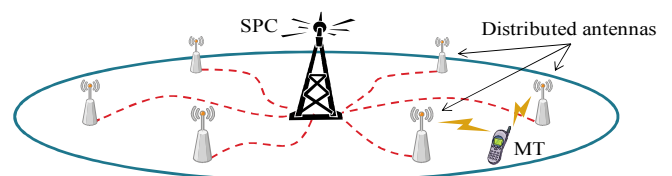


Fig. 1 Conceptual structure of DAN.

II. SC-DAN MODEL AND PROPAGATION MODEL

A. SC-DAN Model

In this paper, the single-user and single-cell SC-DAN is considered. Figure 2 illustrates the DAN antenna distribution. Antennas are uniformly distributed with equal distance R between adjacent antennas. An MT having N_M antennas is randomly located in the shaded area. It is assumed that SPC selects N_D distributed antennas nearest from the MT.

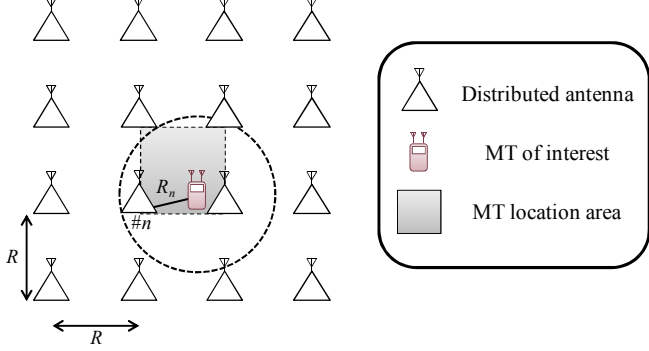


Fig. 2 Antenna distribution.

B. Channel Model

The broadband propagation channel is characterized by distant-dependent path loss, log-normally distributed shadowing loss, and frequency-selective fading. The local average received signal power $P_{r,n}$ at the MT for the signal transmitted from the n -th distributed antenna is given by

$$P_{r,n} = P'_{t,n} \cdot R_n^{-\alpha} \cdot 10^{\frac{\eta_n}{10}} = P_{t,n} \cdot r_n^{-\alpha} \cdot 10^{\frac{\eta_n}{10}}, \quad (1)$$

where $P'_{t,n}$ is the transmit power from the n -th antenna, R_n is the distance between the MT and the n -th distributed antenna, and α and η_n are the path loss exponent and the shadowing loss in dB, respectively. η_n is a zero-mean Gaussian variable with standard deviation σ . In Eq. (1), $P_{t,n} = P'_{t,n} \cdot R^{-\alpha}$ and $r_n = R_n/R$ are respectively the normalized transmit power and the normalized distance. The total transmit power from N_D antennas is kept constant as

$$P_t = \sum_{n=0}^{N_D-1} P_{t,n}. \quad (2)$$

Assuming that frequency-selective fading is composed of L discrete paths, the symbol-spaced channel impulse response between the n -th distributed antenna and the m -th MT antenna can be expressed as

$$h_{m,n}(\tau) = \sqrt{r_n^{-\alpha} \cdot 10^{\frac{\eta_n}{10}}} \cdot \sum_{l=0}^{L-1} h_{m,n,l} \delta(\tau - \tau_l), \quad (3)$$

where $h_{m,n,l}$ and τ_l are the complex-valued channel gain with $E[\sum_{l=0}^{L-1} |h_{m,n,l}|^2] = 1$ and the time delay of the l -th path between the n -th distributed antenna and m -th MT antenna.

III. FD-STBC-JTRC ENCODING/DECODING

Figure 3 illustrates the SC-DAN downlink transmitter/receiver structure. FD-STBC-JTRD encoding/decoding for various combinations of transmit/receive antennas can be found in [12]. We consider a block transmission of $J \times N_c$ data modulated symbols $\{d(t); t=0 \sim JN_c-1\}$. It is assumed that perfect CSI is available at the SPC. FD-STBC-JTRD encoding, decoding, and transmit FDE weights are presented in Sects. III-A, III-B, and III-C, respectively. STBC-JTRD using N_D transmit antennas and N_M receive antennas can achieve an $N_D \times N_M$ -th order (full) diversity gain [10].

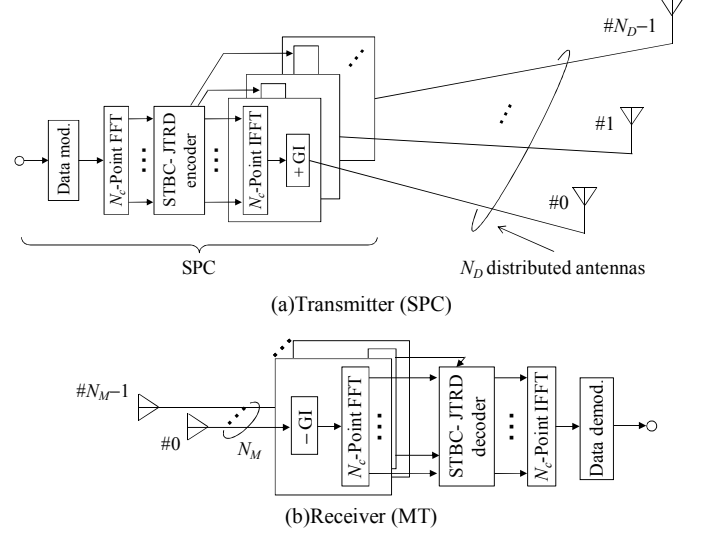


Fig. 3 SC-DAN transmitter/receiver structure using FD-STBC-JTRD.

A. Encoding

At the SPC, a sequence of $J \times N_c$ data modulated symbols to be transmitted is divided into a sequence of J blocks of N_c symbols each. N_c -point fast Fourier transform (FFT) is applied to decompose the j -th symbol block $\{d_j(t); t=0 \sim N_c-1\}$ into the frequency-domain signal $\{D_j(k); k=0 \sim N_c-1\}$ as

$$D_j(k) = \frac{1}{\sqrt{N_c}} \sum_{t=0}^{N_c-1} d_j(t) \exp\left(-j2\pi k \frac{t}{N_c}\right). \quad (4)$$

A sequence of J frequency-domain signals, $\{D_j(k); k=0 \sim N_c-1\}$, $j=0 \sim J-1$, is encoded into N_D streams of Q coded frequency-domain signal blocks each. A combination of J and Q is shown in Table 1 for $N_M=1 \sim 4$. The coding rate $R_s (= J/Q)$ changes from 1 to 3/4 as N_M increases from 1 to 4.

Table 1 Relationship of N_M , J , Q , and code rate R_s

N_M	J	Q	R_s
1	1	1	1
2	2	2	1
3	3	4	3/4
4	3	4	3/4

N_D streams of Q coded frequency-domain signal blocks each can be expressed using a matrix $\mathbf{S}(k)$ of size $N_D \times Q$ as

$$\mathbf{S}(k) = [\mathbf{S}_0(k), \dots, \mathbf{S}_q(k), \dots, \mathbf{S}_{Q-1}(k)] = C_{N_M} \mathbf{W}^H(k) \mathbf{D}_{N_M}(k), \quad (5)$$

where $\mathbf{S}_q(k) = [S_{q,0}(k), \dots, S_{q,n}(k), \dots, S_{q,N_D-1}(k)]^T$ is the k -th frequency component of the q -th encoded frequency-domain signal vector to be transmitted from N_D distributed antennas, $\mathbf{W}(k) = [\mathbf{W}_0(k), \dots, \mathbf{W}_m(k), \dots, \mathbf{W}_{N_M-1}(k)]$ with $\mathbf{W}_m(k) = [W_{m,0}(k), \dots, W_{m,n}(k), \dots, W_{m,N_D-1}(k)]$ is an $N_M \times N_D$ transmit FDE weight matrix (which will be presented in Sect. III-C), $(\cdot)^H$ is the Hermitian transpose, and $\mathbf{D}_{N_M}(k)$ is an encoding matrix of size $N_M \times Q$ which is given as

$$\mathbf{D}_2(k) = \begin{pmatrix} D_0(k) & -D_1^*(k) \\ D_1(k) & D_0^*(k) \end{pmatrix} \quad \dots \text{ for } N_M=2, \quad (6a)$$

$$\mathbf{D}_3(k) = \begin{pmatrix} D_0(k) & -D_1^*(k) & -D_2^*(k) & 0 \\ D_1(k) & D_0^*(k) & 0 & D_2(k) \\ D_2(k) & 0 & D_0^*(k) & -D_1(k) \end{pmatrix} \quad \dots \text{ for } N_M=3, \quad (6b)$$

$$\mathbf{D}_4(k) = \begin{pmatrix} D_0(k) & -D_1^*(k) & -D_2^*(k) & 0 \\ D_1(k) & D_0^*(k) & 0 & D_2(k) \\ D_2(k) & 0 & D_0^*(k) & -D_1(k) \\ 0 & D_2(k) & D_1^*(k) & D_0(k) \end{pmatrix} \quad \dots \text{ for } N_M=4. \quad (6c)$$

C_{N_M} is the power normalization factor, to keep the average transmit power intact, given as

$$C_{N_M} = \frac{N_c}{\sqrt{\sum_{m=0}^{N_M-1} \sum_{n=0}^{N_D-1} \sum_{k=0}^{N_c-1} |W_{m,n}(k)|^2}}. \quad (7)$$

Finally, N_c -point inverse FFT (IFFT) is applied to $\mathbf{S}(k)$ to obtain the time-domain codeword $\{s_{q,n}(t); t=0 \sim N_c-1, q=0 \sim Q-1, n=0 \sim N_D-1\}$, as

$$s_{q,n}(t) = \sqrt{\frac{2P_t}{N_c}} \sum_{k=0}^{N_c-1} S_{q,n}(k) \exp\left(j2\pi k \frac{t}{N_c}\right), \quad (8)$$

where P_t denotes the total transmit power defined in Sect. II. After inserting a cyclic prefix (CP) of N_g symbols into the guard interval (GI), N_D streams of (N_c+N_g) symbol blocks each are transmitted from N_D distributed antennas.

B. Decoding

At the MT receiver, a superposition of N_D transmitted signals is received by N_M antennas. After removing GI, N_M received signals are transformed by N_c -point FFT into the received frequency domain signals $\{R_{q,m}(k); k=0 \sim N_c-1, q=0 \sim Q-1 \text{ and } m=0 \sim N_M-1\}$. The received frequency-domain signals can be expressed using a matrix of size $N_M \times Q$ as

$$\begin{aligned} \mathbf{R}(k) &= [\mathbf{R}_0(k), \dots, \mathbf{R}_q(k), \dots, \mathbf{R}_{Q-1}(k)] \\ &= \sqrt{2P_t} \mathbf{H}(k) \mathbf{S}(k) + \mathbf{N}(k) \end{aligned}, \quad (9)$$

where $\mathbf{R}_q(k) = [R_{q,0}(k), \dots, R_{q,m}(k), \dots, R_{q,N_M-1}(k)]^T$, $\mathbf{H}(k) = [\mathbf{H}_0(k), \dots, \mathbf{H}_m(k), \dots, \mathbf{H}_{N_M-1}(k)]^T$ with $\mathbf{H}_m(k) = [H_{m,0}(k), \dots, H_{m,n}(k), \dots, H_{m,N_D-1}(k)]^T$, and $\mathbf{N}(k) = [\mathbf{N}_0(k), \dots, \mathbf{N}_m(k), \dots, \mathbf{N}_{N_M-1}(k)]^T$ with $\mathbf{N}_m(k) = [N_{m,0}(k), \dots, N_{m,q}(k), \dots, N_{m,Q-1}(k)]$. $H_{m,n}(k)$ represents the channel gain at the k -th frequency given as

$$H_{m,n}(k) = \sqrt{r_n^{-\alpha} \cdot 10^{-\frac{\eta_n}{10}}} \cdot \sum_{l=0}^{L-1} h_{m,n,l} \exp\left(-j2\pi k \frac{\tau_l}{N_c}\right). \quad (10)$$

$\{N_{m,q}(k); m=0 \sim N_M-1, q=0 \sim Q-1\}$ is i.i.d. complex Gaussian variable having zero mean and variance $2N_0N_c/T_s$ with N_0 being single-sided power spectrum density of additive white Gaussian noise (AWGN) and T_s being the symbol period.

The frequency-domain STBC-JTRD decoding is carried out on $\mathbf{R}(k)$ to obtain the decoded frequency domain signal vector $\hat{\mathbf{D}}(k) = [\hat{D}_0(k), \dots, \hat{D}_j(k), \dots, \hat{D}_{J-1}(k)]^T$ as

$$\begin{pmatrix} \hat{D}_0(k) \\ \hat{D}_1(k) \end{pmatrix} = \begin{pmatrix} R_{0,0}(k) + R_{1,1}^*(k) \\ R_{0,1}(k) - R_{1,0}^*(k) \end{pmatrix} \quad \dots \text{ for } N_M=2, \quad (11a)$$

$$\begin{pmatrix} \hat{D}_0(k) \\ \hat{D}_1(k) \\ \hat{D}_2(k) \end{pmatrix} = \begin{pmatrix} R_{0,0}(k) + R_{1,1}^*(k) + R_{2,2}^*(k) \\ R_{0,1}(k) - R_{1,0}^*(k) + R_{2,2}^*(k) \\ R_{0,2}(k) - R_{2,0}^*(k) - R_{3,1}^*(k) \end{pmatrix} \quad \dots \text{ for } N_M=3, \quad (11b)$$

$$\begin{pmatrix} \hat{D}_0(k) \\ \hat{D}_1(k) \\ \hat{D}_2(k) \end{pmatrix} = \begin{pmatrix} R_{0,0}(k) + R_{1,1}^*(k) + R_{2,2}^*(k) + R_{3,3}^*(k) \\ R_{0,1}(k) - R_{1,0}^*(k) - R_{2,3}^*(k) + R_{3,2}^*(k) \\ R_{0,2}(k) + R_{1,3}^*(k) - R_{2,0}^*(k) - R_{3,1}^*(k) \end{pmatrix} \quad \dots \text{ for } N_M=4. \quad (11c)$$

As understood from Eq. (11), FD-STBC-JTRD decoding needs only addition/subtraction and conjugate operations. Finally, N_c -point IFFT is applied to transform $\{\hat{D}_j(k)\}$ into the time-domain soft decision symbol as

$$\hat{d}_j(t) = \frac{1}{\sqrt{N_c}} \sum_{k=0}^{N_c-1} \hat{D}_j(k) \exp\left(j2\pi k \frac{t}{N_c}\right). \quad (12)$$

C. Transmit FDE Weight

The MMSE transmit FDE $\mathbf{W}_m(k) = [W_{m,0}(k), \dots, W_{m,n}(k), \dots, W_{m,N_D-1}(k)]$ minimizes the mean square error (MSE) between $D_j(k)$ and $\hat{D}_j(k)$. Following [12], $W_{m,n}(k)$ can be derived as

$$W_{m,n}(k) = \frac{\left(\frac{P_r T_s}{N_0}\right) H_{m,n}(k)}{\frac{1}{N_M} \frac{P_r T_s}{N_0} \sum_{n=0}^{N_D-1} \sum_{m=0}^{N_M-1} |H_{m,n}(k)|^2 + 1}. \quad (13)$$

IV. COMPUTER SIMULATION

A. Simulation Conditions

Simulation conditions are summarized in Table 2. The simulation procedure is as follows: Firstly, the location of the MT is generated in the shaded area in Fig. 2. Secondly, the channel impulse responses $\{h_{m,n}(\tau)\}$ between distributed transmit antennas and MT receive antennas are generated. Then, the downlink transmissions using FD-STBC-JTRD are performed to measure the instantaneous BER with the constant transmit $E_s/N_0 (= P_r T_s)$. The above steps are repeated sufficient number of times to obtain the BER distribution.

Table 2 Simulation condition

Data modulation	QPSK
No. of FFT points	$N_c=256$
Guard interval length	$N_g=32$
No. of distributed antennas	$N_D=1, 2, 3, 4$
No. of MT antennas	$N_M=1, 2$
Channel estimation	Ideal
Transmit FDE weight	MMSE
Normalized total transmit E_s/N_0	$E_s/N_0=5$ (dB)
No. of paths	$L=1, 2, 4, 16$
Power delay profile	Uniform
Time delay	$\tau_l=l$
Path loss exponent	$\alpha=3.5$
Shadowing loss standard derivation	$\sigma=3.0, 5.0, 7.0$

B. Impacts of N_D And N_M

Figure 5 plots the complementary cumulative distribution function (CCDF) of the measured BER for various combinations of N_D and N_M . It can be seen that by increasing N_D , the BER can be significantly reduced since the received signal power drops due to the path loss, shadowing loss, and frequency-selective fading can be better suppressed. When $N_M=1$, the BER level which the measured BER exceeds at the 1% probability (this is called the 1% outage BER in this paper) is 2×10^{-1} , 4×10^{-2} , 8×10^{-3} , and 2×10^{-3} for $N_D=1, 2, 3$ and 4, respectively.

For a fixed number of N_D , the 1% outage BER can be reduced by increasing N_M because of a larger receive diversity gain. However, Fig. 5 indicates that increasing the number of distributed transmit antennas, N_D , can more reduce the 1%

BER than increasing the number of MT receive antennas, N_M ; the comparison of $(N_D, N_M)=(2, 1)$ and $(N_D, N_M)=(1, 2)$ shows that the former achieves lower 1% outage BER than the latter. This is because only addition/subtraction and conjugate operations are performed at MT for decoding without CSI. Therefore, the received signal-to-noise ratio (SNR) after decoding is smaller by a factor of $1/N_M$ than coherent maximal ratio combining (MRC). The conditional SNR for the given channel condition is expressed as (derivation is omitted for the sake of brevity)

$$\gamma\left(\frac{E_s}{N_0}, \{H_{m,n}(k)\}\right) = \frac{2}{N_M} \left(\frac{E_s}{N_0}\right) \sum_{m=0}^{N_M-1} \sum_{n=0}^{N_D-1} (r_n^{-\alpha} \cdot 10^{\frac{\eta_n}{10}}) \sum_{l=0}^{L-1} |h_{m,n,l}|^2. \quad (14)$$

Eq. (14) clearly shows that increasing the value of N_D consistently increases the average received SNR while the average SNR is kept the same irrespective of N_M .

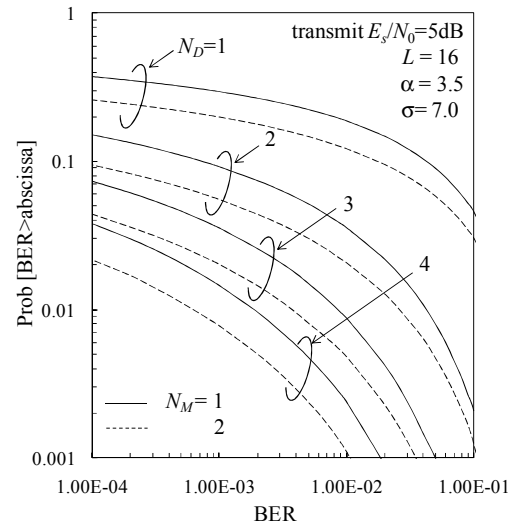


Fig. 5 Impact of the number of transmit (SPC) and receive (MT) antennas, N_D and N_M .

C. Impacts of The Propagation Parameters

Figure 6 plots the CCDF of the measured BER with the number of paths, L , as a parameter for $(N_D, N_M)=(4, 2)$. As L increases, the channel frequency-selectivity gets stronger. This can be exploited by the transmit FDE to reduce the BER outage probability.

Figure 7 illustrates the CCDF of the measured BER with shadowing standard deviation σ as a parameter for $(N_D, N_M)=(4, 2)$. It can be seen from Fig. 7 that the BER outage probability significantly decreases as σ decreases. The shadowing loss has a big impact on the BER performance. An introduction of DAN antenna selection based on the short term SNR (i.e., based on path loss and shadowing loss) may improve the performance more. The impact of antenna selection criterion is left as an important future study.

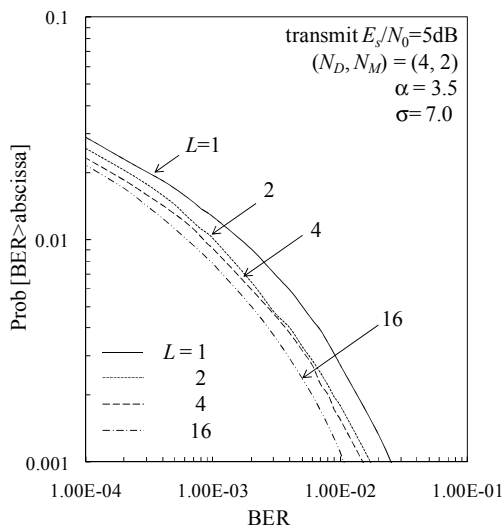


Fig. 6 Impact of the number of propagation paths, L .

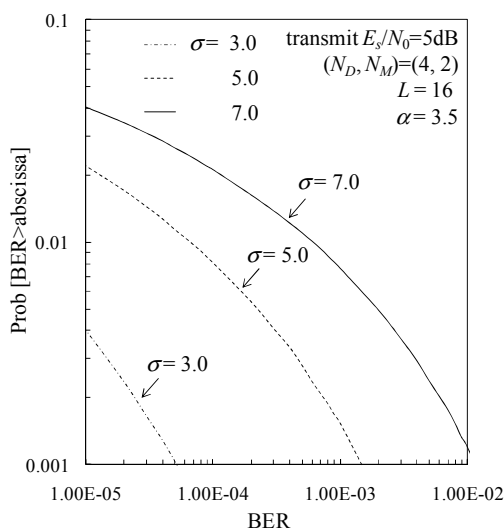


Fig. 7 Impact of the shadowing standard deviation, σ .

V. CONCLUSION

In this paper, we evaluated the BER outage probability of SC-DAN downlink using FD-STBC-JTRD. FD-STBC-JTRD allows the use of an arbitrary number of distributed transmit antennas. We showed that the BER outage probability can be significantly reduced by increasing the number of distributed antennas while keeping MT receiver's complexity low.

We assumed a distance based distributed transmit antenna selection. It was shown that the shadowing loss has a big impact on the BER performance. An introduction of distributed antenna selection based on the short term SNR may improve the performance more. Selection criterion of distributed transmit antennas is an important future study. In downlink transmission, an arbitrary number of distributed transmit antennas can be used while limiting the number of MT receive antennas. For uplink transmission, FD-STTD can

be applied to use an arbitrary number of distributed receive antennas while limiting the number of MT transmit antennas. A performance comparison of SC-DAN downlink using FD-STBC-JTRD and uplink using FD-STTD is also left as an important future study.

REFERENCES

- [1] W. C. Jakes, Jr., Ed., *Microwave Mobile Communications*. Wiley, New York, 1974.
- [2] D. Falconer, S. L. Ariyavisitakul, A. Benyamin-Seeyar, and B. Eidson, "Frequency domain equalization for single-carrier broadband wireless systems," *IEEE Commun. Mag.*, vol.40, no. 4, pp. 58-66, Apr. 2002.
- [3] F. Adachi, T. Sao and T. Itagaki, "Performance of multicode DS-SS using frequency domain equalization in a frequency selective fading channel," *IEE Electronics Letters*, vol. 39, No.2, pp. 239-241, Jan. 2003.
- [4] R. L. U Choi and R. D. Murch, "A transmit MIMO scheme with frequency domain pre-equalization for wireless frequency selective channels," *IEEE Trans. Wireless Commun.*, Vol. 3, No. 3, pp. 929-938, May 2004.
- [5] Y. Zhu and K. B. Letaief, "Frequency Domain Pre-Equalization with Transmit Precoding for MIMO Broadcast Wireless Channels," *IEEE Trans. Wireless Commun.*, Vol. 26, No. 2, pp. 389-400, Feb. 2008.
- [6] H. Sari and F. Buda, "Characteristics and Compensation of Multipath Propagation in Broadband Wireless Access System," *ECPS 2005 Conference*, 15-18 Mar. 2005.
- [7] A. Gusmao, R. Dinis and N. Esteves, "On Frequency-Domain Equalization and Diversity Combining for Broadband Wireless Communications," *IEEE Trans Wireless Commun.*, Vol. 51, No. 7, pp. 1029-1033, Jul. 2003.
- [8] F. Adachi and K. Takeda, "Bit Error Rate Analysis of DS-SS with Joint Frequency-Domain Equalization and Antenna Diversity Combining," *IEICE Trans. Commun.*, Vol. E87-B, No.10, pp.2991-3002, Oct. 2004.
- [9] K. Takeda, T. Itagaki, and F. Adachi, "Application of space-time transmit diversity to single-carrier transmission with frequency-domain equalization and receive antenna diversity in a frequency-selective fading channel," *IEE Proc.-Commun.*, vol. 151, No.6, pp. 627-632, Dec. 2004.
- [10] H. Tomeba, K. Takeda and F. Adachi, "Space-Time Block Coded Joint Transmit/Receive Diversity in a Frequency-Nonselective Rayleigh Fading Channel," *IEICE Trans. Commun.*, Vol.E89-B, No.8, pp.2189-2195, Aug. 2006.
- [11] H. Tomeba, K. Takeda, and F. Adachi, "Space-Time Block Coded-Joint Transmit/Receive Antenna Diversity using more than 4 Receive Antennas," *2008 IEEE 68th Vehicular Technology Conference (VTC-Fall)*, Calgary, Canada, 21-25 September 2008.
- [12] H. Tomeba and F. Adachi, "Frequency-domain Space-Time Block Coded-Joint Transmit/Receive Diversity for The Single Carrier Transmission," *Proc.10th IEEE International Conference on Communication Systems (ICCS 2006)*, Singapore, 30 Oct. - Nov. 2006.
- [13] A. Goldsmith, *Wireless Communications*, Cambridge University Press, 2005.
- [14] W. Choi, J. G. Andrews and C. Yi, "The Capacity of Multicellular Distributed Antenna Networks", *IEEE Wirelesscom, Information theory symposium*, Jun. 2005.
- [15] W. Choi, "Downlink performance and capacity of distributed antenna systems," *IEEE Trans. Wireless Commun.*, Vol. 6, No. 1, pp. 69-73, Jan. 2007.
- [16] H. Matsuda, H. Tomeba and F. Adachi, "Channel Capacity of Distributed Antenna System Using Maximal Ratio Transmission," *The 5th IEEE VTS Asia Pacific Wireless Communications Symposium (APWCS 2008)*, Tohoku University, Sendai, Japan, 21-22 Aug. 2008.